The mTOR pathway is regulated by polycystin-1, and its inhibition reverses renal cystogenesis in polycystic kidney disease

Jonathan M. Shillingford*†, Noel S. Murcia†‡, Claire H. Larson§, Seng Hui Low*, Ryan Hedgepeth¶, Nicole Brown‡, Chris A. Flask‖, Andrew C. Novick¶, David A. Goldfarb¶, Albrecht Kramer-Zucker**, Gerd Walz**, Klaus B. Piontek††, Gregory G. Germino††, and Thomas Weimbs*‡‡

*Department of Molecular, Cellular, and Developmental Biology, University of California, Santa Barbara, CA 93106-9610; §Department of Cell Biology, Lerner Research Institute, and ¶Glickman Urological Institute, The Cleveland Clinic, Cleveland, OH 44195; Departments of ‡Pediatrics, ‖Radiology, and Biomedical Engineering, Case Western Reserve University, Cleveland, OH 44106; **Division of Nephrology, Department of Medicine, University Hospital Freiburg, 79106 Freiburg, Germany; and ††Department of Medicine, Johns Hopkins University School of Medicine, Baltimore, MD 21205

Edited by John A. Carbon, University of California, Santa Barbara, CA, and approved February 8, 2006 (received for review November 7, 2005)

Autosomal-dominant polycystic kidney disease (ADPKD) is a common genetic disorder that frequently leads to renal failure. Mutations in polycystin-1 (PC1) underlie most cases of ADPKD, but the function of PC1 has remained poorly understood. No preventive treatment for this disease is available. Here, we show that the cytoplasmic tail of PC1 interacts with tuberin, and the mTOR pathway is inappropriately activated in cyst-lining epithelial cells in human ADPKD patients and mouse models. Rapamycin, an inhibitor of mTOR, is highly effective in reducing renal cystogenesis in two independent mouse models of PKD. Treatment of human ADPKD transplant-recipient patients with rapamycin results in a significant reduction in native polycystic kidney size. These results indicate that PC1 has an important function in the regulation of the mTOR pathway and that this pathway provides a target for medical therapy of ADPKD.

rapamycin | renal epithelial cells | tuberin

Autosomal-dominant polycystic kidney disease (ADPKD) is one of the most common human monogenic diseases and affects 12 million people worldwide (for recent reviews, see refs. 1–5). Excessive proliferation of renal epithelial cells leads to cysts that eventually replace most of the normal tissue. Consequently, ADPKD results in severe enlargement of the kidneys, and renal failure occurs in most cases by the age of 50. Survival depends on lifelong hemodialysis or kidney transplantation. No alternative clinical treatment is currently available.

Mutations in the *PKD1* gene, which encodes PC1, account for >85% of ADPKD cases. PC1 is a multispanning membrane protein with a C-terminal cytoplasmic tail of ≈226 residues. The PC1 tail has been implicated in several signaling pathways (5). Recent evidence suggests that PC1 may also play a role in cilia-mediated sensing of luminal fluid flow by renal epithelial cells (6). Which of these proposed functions are critical for renal cyst formation is unknown. Mutations in several genes unrelated to PC1 can also lead to a renal cystic phenotype in animal models and humans, but it is unclear whether all of these genotypes may converge on a common pathway that is critical for cyst formation. If such a common pathway exists, it would provide an excellent target for treatment strategies.

We have focused on the possibility that PC1 may act in a common pathway with tuberin, the product of the *TSC2* gene. *TSC2* mutations lead to tuberous sclerosis, a disease characterized by renal cysts and benign tumors in multiple organs (7, 8). Whereas upstream events that regulate tuberin are poorly understood, its ability to regulate the kinase activity of mTOR, via the small GTPase rheb (9), has recently been described (10, 11). mTOR has essential roles in protein translation (12, 13), cell growth, and proliferation and is up-regulated in several types of tumors (14). A possible role of mTOR in renal cystic disease is supported by two recent reports indicating that an inhibitor of mTOR slows disease progression in the Han:SPRD rat model (15, 16).

Here, we report that the C-terminal cytoplasmic tail of PC1 interacts with tuberin. The mTOR pathway is inappropriately activated in cyst-lining epithelial cells in human ADPKD and three mouse models with different affected genes, suggesting that this is a common, convergent event during renal cystogenesis. Rapamycin is a clinically approved drug and a specific mTOR inhibitor. We found that rapamycin is highly effective in reducing cystogenesis in two PKD mouse models and also leads to a significant reduction of renal size in end-stage ADPKD patients after renal transplantation. These results indicate that dysregulation of mTOR underlies changes in renal epithelial cells that cause the formation of polycystic kidneys in multiple genetic backgrounds. These results also provide a mechanistic link among PC1, tuberin, and mTOR, suggesting that rapamycin and related drugs that target the mTOR pathway are excellent candidates for a therapeutic approach to prevent or delay the onset of PKD.

Results

The Cytoplasmic Tail of PC1 Interacts with Tuberin and mTOR. To investigate signaling functions mediated by the cytoplasmic tail of PC1 in a model system relevant to renal epithelial cell biology, we generated stable clones of the Madin–Darby canine kidney (MDCK) cell line, which has been shown to express endogenous PC1 (17, 18) and is, therefore, likely to possess the components involved in downstream signaling pathways. Cells were engineered to stably express membrane-anchored fusion proteins of the entire cytoplasmic tail of PC1 (FLM-PC1) or the N-terminal (NTM-PC1) or C-terminal (CTM-PC1) half of the tail in a doxycycline (DOX)-inducible manner. Expression of NTM-PC1 containing the membrane-proximal 92 residues of the PC1 tail resulted in cell cycle arrest after 24 h and apoptosis at 48 h after induction of expression (see Fig. 6, which is published as supporting information on the PNAS web site). Expression of FLM-PC1 or CTM-PC1 had no similar effects on apoptosis (data not shown). Because increased apoptosis is a hallmark of cystic epithelial cells in ADPKD, these results suggested that expression of NTM-PC1 might affect a downstream pathway of PC1 that is relevant to renal cystogenesis.

To investigate the possibility that the effect induced by NTM-PC1 may involve tuberin, we determined the subcellular localization of

Conflict of interest statement: No conflicts declared.

This paper was submitted directly (Track II) to the PNAS office.

Abbreviations: ADPKD, autosomal-dominant polycystic kidney disease; DOX, doxycycline; H&E, hematoxylin and eosin; MDCK, Madin–Darby canine kidney.

†J.M.S. and N.S.M. contributed equally to this work.

‡‡To whom correspondence should be addressed. E-mail: weimbs@lifesci.ucsb.edu.

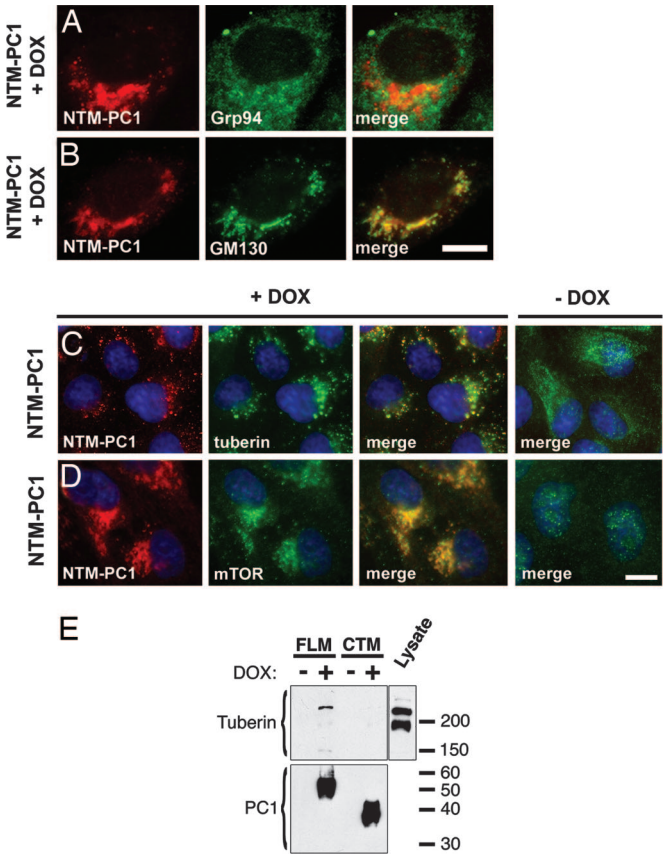

Fig. 1. The N-terminal cytoplasmic domain of PC1 (NTM-PC1) colocalizes with mTOR and colocalizes and interacts with tuberin. (*A–D*) Expression of NTM-PC1 was induced with DOX for 16 h before fixation and immunostaining with antibodies against the indicated proteins. Noninduced NTM-PC1 cells served as controls (*C* and *D*, −DOX). Grp94 and GM130 are resident proteins of the endoplasmic reticulum and Golgi apparatus, respectively. (*E*) FLM-PC1 and CTM-PC1 cells were cultured in the absence or presence of DOX for 16 h, the PC1 fusion proteins were immunoprecipitated by using an antibody against CD16, and binding proteins were analyzed by Western blot with the indicated antibodies. The starting material (MDCK lysate) serves as a control. [Scale bars, 3 μm (*A–D*).]

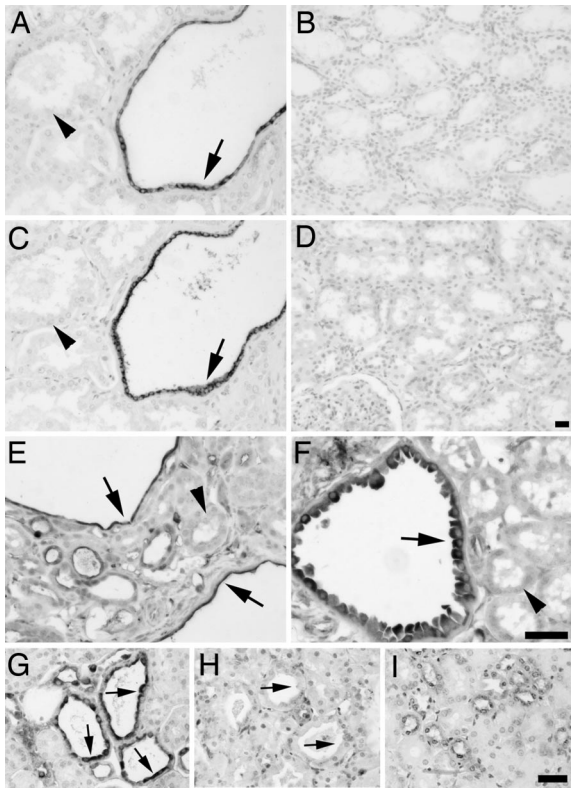

Fig. 2. Phospho-mTOR, -S6K, and -S6 are specifically induced in cyst-lining epithelial cells in ADPKD and mouse models. (*A–D*) Renal tissue sections isolated from human ADPKD patients (*A* and *C*) or normal patients (*B* and *D*) were analyzed by immunohistochemistry using antibodies against phospho-mTOR (Ser 2448) (*A* and *B*) or phospho-S6K (Thr 389) (*C* and *D*). Note specific staining of cystic epithelial cells (*A* and *C*, arrows) but not surrounding normal epithelium (*A* and *C*, arrowheads). (*E–I*) Renal tissue sections derived from *Pkd1*$^{cond/cond}$:TgN(balancer1)2Cgn (*E*) and MAL-overexpressing (*F*) mice, nontreated (*G*) or rapamycin-treated (*H*) (5 mg/kg of body weight) *oprk*-rescue (*Tg737*$^{orpk/orpk}$;*TgRsq*) mutant mice, and nontreated *orpk*-heterozygous-rescue (*Tg737*$^{orpk/+}$;*TgRsq*) (*I*) control mice were immunostained by using an antibody against phospho-S6 ribosomal protein (Ser 235/236). Note specific cytoplasmic staining of cystic-epithelial cells (*E–G*, arrows) but not surrounding normal epithelium (*E* and *F*, arrowheads; and *I*). The cyst-specific cytoplasmic immunosignal is abolished after rapamycin treatment (*H*, arrows). (Scale bars, 20 μm.)

tuberin in cells that were induced to express NTM-PC1 for 16 h, a time point before detectable effects on apoptosis or the cell cycle. As shown in Fig. 1*B*, NTM-PC1 itself localizes mainly to the Golgi apparatus. Whereas tuberin exhibits punctate cytoplasmic localization in control cells (Fig. 1*C*, −DOX), expression of NTM-PC1 caused significant retargeting of tuberin to the Golgi apparatus, where it now colocalizes with NTM-PC1 (Fig. 1*C*, +DOX). In contrast, expression of CTM-PC1 did not result in Golgi localization of tuberin (data not shown). The observed "forced" colocalization of tuberin with NTM-PC1 suggested that these two proteins may interact.

To assess this possible interaction biochemically, FLM-PC1 was immunoprecipitated from MDCK lysates, and binding proteins were analyzed by Western blot. As shown in Fig. 1*E*, endogenous tuberin coprecipitates with FLM-PC1, but not CTM-PC1, in a DOX-dependent manner. A faster-migrating band visible in the total lysate likely represents a splice isoform of tuberin, which has been reported in human and mouse (19). This form, however, fails to bind to the PC1 tail, suggesting that sequences missing in this isoform may be critical for PC1 binding.

Because mTOR is a known downstream effector of tuberin, we next investigated mTOR localization in NTM-PC1 cells. Confocal immunofluorescence microscopy revealed that mTOR also undergoes retargeting and colocalization with NTM-PC1 at the Golgi apparatus (Fig. 1*D*), suggesting that mTOR, possibly through its interaction with the rheb–tuberin complex (20), may be part of a multicomponent complex recruited by PC1.

The mTOR Pathway Is Inappropriately Activated in Cystic Epithelial Cells in Human ADPKD and Mouse Models. These data raised the possibility that mTOR may be regulated by PC1. To test this hypothesis, we made use of the availability of human tissue and mouse models in which PC1 is inactivated. Kidney tissue sections from ADPKD patients and normal controls were investigated by using antibodies against the phosphorylated, active forms of mTOR and its downstream effector S6 kinase. As shown in Fig. 2*A*, cyst-lining epithelial cells (arrows), but not surrounding normal epithelium (arrowheads) or normal tissue (Fig. 2*B*), exhibit intense cytoplasmic staining of phospho-mTOR (Ser 2448), indicative of elevated mTOR activity. Similarly, the same cyst-lining epithelial cells (Fig. 2*C*, arrows) exhibit highly elevated levels of phospho-S6 kinase (Thr 389), a surrogate marker of mTOR pathway activity, as compared with surrounding normal epithelium (Fig. 2*C*, arrowheads) or control kidney (Fig. 2*D*). Similar staining was observed

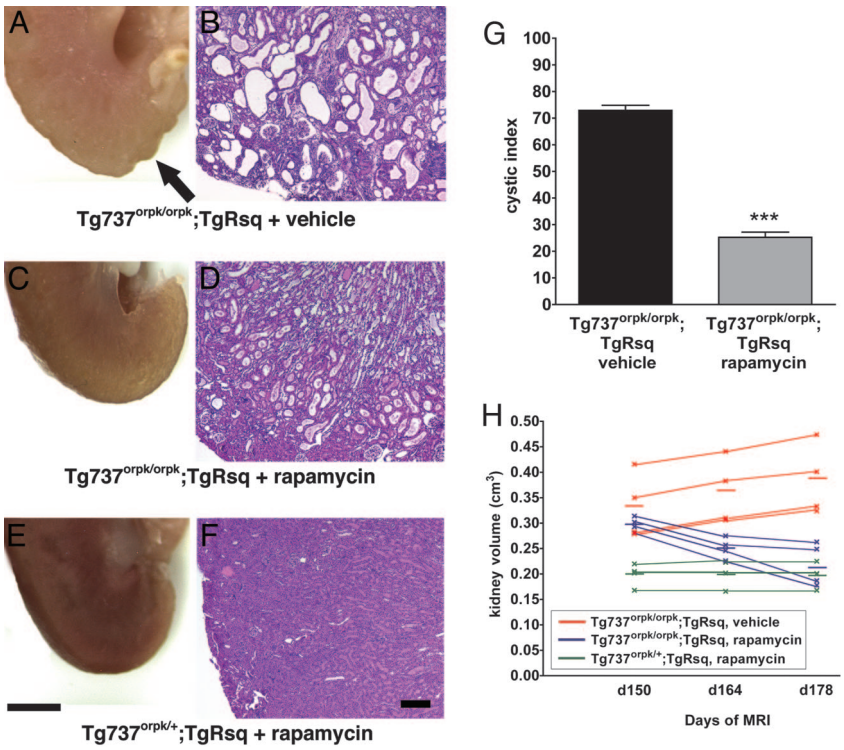

Fig. 3. Rapamycin treatment significantly improves renal cystogenesis in the *orpk*-rescue mouse model. Day-150 postpartum *orpk*-rescue (*Tg737*$^{orpk/orpk}$;*TgRsq*) mutant mice and *orpk*-heterozygous-rescue (*Tg737*$^{orpk/+}$;*TgRsq*) control mice were given daily i.p. injections of rapamycin (5 mg/kg of body weight) or vehicle for 28 days before isolation, fixation, and sectioning of whole kidneys. (*A–F*) Representative whole kidney (*A*, *C*, and *E*) and H&E-stained sections (*B*, *D*, and *F*) derived from non-rapamycin-treated (*A* and *B*) or rapamycin-treated (*C* and *D*) (5 mg/kg of body weight) *orpk*-rescue mutant mice and *orpk*-heterozygous-rescue (*E* and *F*) control mice. Note the nonuniform appearance of the nontreated mutant kidney (*A*, arrow) compared with the smooth surface of the treated mutant kidney (*C*). (*G*) Cystic indices were calculated based on representative renal sections derived from non-rapamycin-treated and rapamycin-treated *orpk*-rescue mutant mice as described in *Materials and Methods*. (*H*) Kidney volumes were measured by MRI scanning of live animals at the beginning (day 150 postpartum), middle (day 164 postpartum), and end (day 178 postpartum) of treatment with rapamycin or vehicle. Each individual line represents a separate kidney for each respective genotype, and the averages for each group are indicated with horizontal lines. [Scale bars, 3 mm (*A*, *C*, and *E*) and 200 μm (*B*, *D*, and *F*).] ***, $P < 0.001$.

in five additional ADPKD cases (data not shown). These results provide evidence that dysregulation of the mTOR pathway is a biochemical feature of renal lesions in human ADPKD patients.

Because available human ADPKD specimens represent advanced stage disease, we further tested whether earlier cystic lesions in a mouse model of PKD exhibit increased mTOR pathway activity. Immunostaining of kidney sections derived from 5-week-old mice that had undergone targeted recombination of the *Pkd1* gene (21) (Fig. 2*E*) revealed that phospho-S6 ribosomal protein (Ser 235/236), a correlate of mTOR activity, is detected specifically in the cyst-lining epithelial cells (arrows) but not surrounding normal epithelium (arrowheads). To determine whether mTOR activation during cystic progression may be a general feature of PKD, we next examined the status of the mTOR pathway in polycystic mouse models independent of *Pkd1* mutations. Mice overexpressing the myelin and lymphocyte (MAL) protein present with PKD (22) and, interestingly, cyst-lining renal epithelial cells exhibited specific cytoplasmic staining of phospho-S6 ribosomal protein (Fig. 2*F*, arrow) compared with surrounding normal epithelium (Fig. 2*F*, arrowhead). The *orpk*-rescue model, in which the cilia protein polaris is defective, results in the manifestation of a late-onset form of PKD reminiscent of human ADPKD (23). *Orpk*-rescue (*Tg737*$^{orpk/orpk}$;*TgRsq*) mutant mice exhibited intense cytoplasmic labeling of cyst-lining epithelial cells by using the phospho-S6 ribosomal protein antibody (Fig. 2*G*, arrows). Strikingly, rapamycin-treated *orpk*-rescue mutant mice (Fig. 2*H*, arrows) showed no evidence of cytoplasmic staining in cysts, demonstrating the effectiveness of rapamycin treatment and the specificity of the immunosignal. Renal sections derived from *orpk*-heterozygous-rescue (*Tg737*$^{orpk/+}$;*TgRsq*) control mice were devoid of significant cytoplasmic staining (Fig. 2*G*). Taken together, these results indicate that mTOR activity is significantly up-regulated in cyst-lining epithelial cells and suggest that this may be a common characteristic of renal cysts caused by defects in several genes whose functions may ultimately converge on this pathway.

Inhibition of mTOR Alleviates the Cystic Phenotype in PKD Mouse Models. If the abnormally high activity of mTOR in renal cystic cells contributes to cyst-formation, then compounds that inhibit mTOR should alleviate renal cystogenesis. Rapamycin is a specific inhibitor of mTOR kinase activity (24, 25). We tested the effect of rapamycin on two mouse models that exhibit late- and early-onset renal cystic phenotypes, respectively. The *orpk*-rescue mouse model described above served as a model of late-onset ADPKD, whereas the *bpk* mouse model (26) served as a model of early-onset ARPKD.

Orpk-rescue (*Tg737*$^{orpk/orpk}$;*TgRsq*) mutant mice and *orpk*-heterozygous-rescue (*Tg737*$^{orpk/+}$;*TgRsq*) control mice were treated with rapamycin (5 mg/kg of body weight per day) starting at postnatal day 150 through day 178. This treatment profoundly improved the cystic phenotype in the mutant mice (Fig. 3*A–D*). The histological cystic index was significantly reduced in rapamycin-treated mutant mice (Fig. 3*G*). To determine whether rapamycin acts mainly by preventing the formation of renal cysts or by a reversal of cystogenesis we measured the total renal volumes by MRI during the course of drug treatment. It has been shown that the degree of cystogenesis correlates with kidney volume (27). Whereas nontreated mutant animals exhibited a 13% increase in renal volume between days 150 and 178, rapamycin-treated animals exhibited a decrease of 30% (Fig. 3*H*; and see Fig. 7, which is published as supporting information on the PNAS web site). Rapamycin had no effect on renal volumes of control mice (Fig. 3*H*). This result suggests that rapamycin effects a reversal of the renal cystic phenotype, possibly in conjunction with inhibition of cystogenesis.

The *bpk* mouse model is characterized by an embryonic onset reminiscent of human ARPKD, and the mice generally fail to live >25 days (26). Rapamycin treatment (5 or 1.67 mg/kg of body weight per day) from day 7 postpartum for a period of 14 days resulted in strong inhibition of the renal cystic phenotype as reflected by a significant decrease (76.6% for 5 mg/kg of body weight per day treatment; 68.7% for 1.67 mg/kg of body weight per day treatment, $n = 4$) in kidney weight as compared with vehicle-treated *bpk* mutant littermates (Fig. 4*D*). Rapamycin-treated *bpk* mutant mice exhibited significantly smaller cyst sizes (Fig. 4 *A–C*) and an improved renal cystic index (Fig. 4*E*) compared with controls. Furthermore, either dose of rapamycin resulted in a

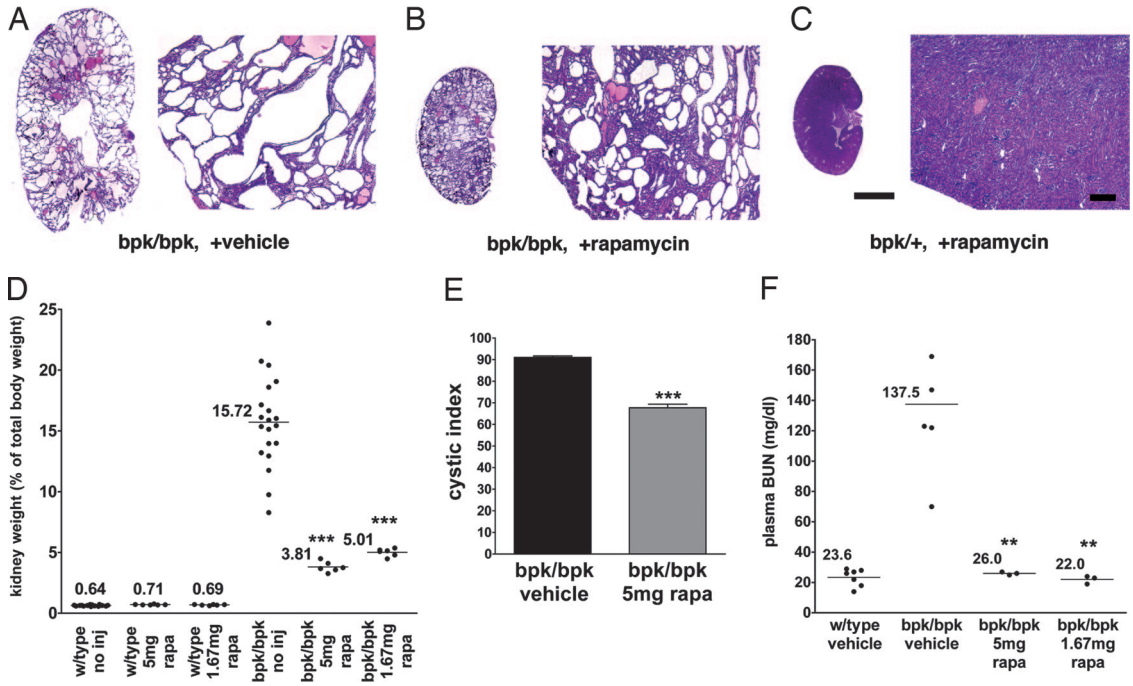

Fig. 4. Rapamycin treatment significantly improves the renal cystic phenotype and kidney function in the *bpk* mouse model. Mutant (*bpk*/*bpk*) and control (*bpk*/+) mice received daily i.p. injections of rapamycin (5 or 1.67 mg/kg of body weight) starting at day 7 for a period of 14 days. (*A–C*) Representative low-power (*Left*) and high-power (*Right*) H&E-stained sections derived from non-rapamycin-treated (*A*) or rapamycin-treated (*B*) (5 mg/kg of body weight) *bpk*/*bpk* mutant and *bpk*/+ (*C*) animals. (*D*) Kidney weight expressed as a percentage of total body weight. (*E*) Cystic indices were calculated based on representative renal sections derived from non-rapamycin-treated and rapamycin-treated *bpk*/*bpk* mutant mice ($n = 4$ kidneys) as described in *Materials and Methods*. (*F*) Blood drawn from anesthetized animals was assayed for blood urea nitrogen (BUN) according to standard procedures. [Scale bars, 3 mm (*A–C*, whole kidney H&E) and 200 μm (*A–C*, histology H&E).] ***, $P < 0.001$; **, $P < 0.01$.

normalization of plasma blood urea nitrogen levels (Fig. 4*F*), an indicator of renal function.

Taken together, these results demonstrate that mTOR inhibition by rapamycin has a significant beneficial effect on renal cystic disease in two independent mouse models, suggesting that mTOR activity is critical for cystogenesis.

Rapamycin Treatment Induces Apoptosis of Cystic Epithelial Cells. Cystic epithelial cells in PKD are generally characterized by an increased rate of both apoptosis and proliferation, which indicates a high cell turnover (1–4). Because rapamycin treatment appeared to not only prevent the onset of cyst formation but also effected a reduction in renal volume, we investigated whether apoptosis may be a mechanism underlying this reduction. As shown in Fig. 5*A*, rapamycin-treated *orpk*-rescue (*Tg737*$^{orpk/orpk}$;*TgRsq*) mutant mice exhibited increased numbers of TUNEL-positive cyst-lining epithelial cells and the presence of luminal TUNEL-positive cells (Fig. 5*A Lower*) as compared with nontreated *orpk*-rescue mutant mice (Fig. 5*A Upper*). Quantification (Fig. 5*B*; and see *Materials and Methods*) revealed a significant ($P < 0.001$, $n = 4$) increase in cyst-lining and luminal TUNEL-positive cells per cyst in rapamycin-treated *orpk*-rescue mutant mice when compared with vehicle-treated *orpk*-rescue mutant mice. These results suggest that rapamycin reduces renal cysts, at least partially, through the selective induction of apoptosis and luminal shedding of cyst-lining epithelial cells in the *orpk*-rescue mutant mouse model.

Rapamycin Treatment After Renal Transplantation Reduces the Size of Affected Kidneys in ADPKD Patients. To determine the possible clinical relevance of our findings, we performed a retrospective study. Advanced-stage ADPKD patients frequently receive a renal transplant without removal of the affected cystic kidneys. Rapamycin treatment is used in some of these patients as an immunosuppressant to prevent transplant rejection (28). We hypothesized that the drug may also have a beneficial effect on the remaining polycystic kidneys. The criteria used to select these patients were that (*i*) they retained one or both of their native polycystic kidneys, (*ii*) they had an initial CT scan no more than 12 months before or 5 months after kidney transplantation, and (*iii*) they had a follow-up CT scan at least 11 months or later after transplantation. The control group, which satisfied these same criteria, consisted of patients receiving adjunct immunosuppression using compounds other than rapamycin. Total kidney volumes were determined by quantification of CT scans.

As shown in Table 1 (which is published as supporting information on the PNAS web site), the rapamycin group showed a statistically significant ($P < 0.001$) decrease in kidney volumes by 24.8 ± 9.7% over an average period of 24 months. In contrast, the control group exhibited a decrease of only 8.6 ± 11.2% in renal volume over an average period of 40 months, which was not statistically significant. There was a statistically significant difference between the rapamycin and the nonrapamycin groups ($P = 0.03$). Considering that the dose of rapamycin administered to transplant patients is significantly lower than what was used in the above animal experiments, these results suggest that rapamycin may have a similar beneficial effect in human ADPKD as we find in the mouse models.

Discussion

In this study, we show that the membrane-proximal half of the cytoplasmic tail of PC1 interacts with a component of the tuberous sclerosis complex, tuberin, and with the kinase mTOR, which is regulated by tuberin. We show that the mTOR pathway is inappropriately activated in cyst-lining epithelial cells in ADPKD patients, most of whom will have mutations in the *PKD1* gene. Together, these results are consistent with a model in which PC1,

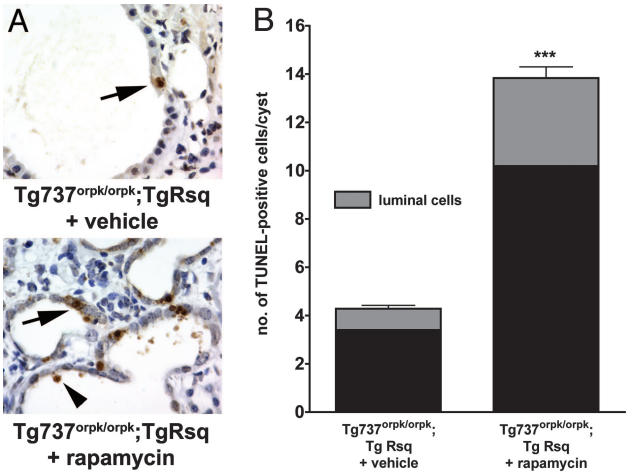

Fig. 5. Rapamycin treatment induces increased apoptosis and luminal shedding of cystic epithelial cells. *Orpk*-rescue (*Tg737*$^{orpk/orpk}$;*TgRsq*) mutant and *orpk*-heterozygous-rescue (*Tg737*$^{orpk/+}$;*TgRsq*) control mice were treated with rapamycin or vehicle as indicated. Renal tissue sections were processed and analyzed for the presence of apoptotic cells by TUNEL. (*A*) TUNEL-positive, cyst-lining epithelial cells were observed in sections of nontreated *Tg737*$^{orpk/orpk}$;*TgRsq* mutant mice, whereas a significant increase in TUNEL-positive, cyst-lining and cyst-luminal epithelial cells were observed in sections of rapamycin-treated *Tg737*$^{orpk/orpk}$;*TgRsq* mutant mice. (*B*) Quantification of TUNEL-positive cells in renal sections derived from vehicle or rapamycin-treated *orpk*-rescue mutant animals expressed as an average of TUNEL-positive cells per cyst ($n = 4$ kidneys). ***, $P < 0.001$.

tuberin, and mTOR form a protein complex in renal epithelial cells, the function of which is the down-regulation of mTOR activity under normal conditions. This hypothesis is further supported by our findings that expression of NTM-PC1 in MDCK cells causes G1-cell cycle arrest and apoptosis. Inhibition of mTOR activity has been shown to lead to G1-cell cycle arrest and apoptosis (29–31). NTM-PC1 therefore might act as a constitutively active inhibitor of mTOR, possibly because of induced proximity to tuberin and/or to sequestration away from its substrates.

Based on studies in a tuberin-deficient cell line, it has been suggested that the expression of tuberin may be required for the targeting of PC1 to the plasma membrane (32). Together with our finding of an interaction between PC1 and tuberin, this may suggest that both proteins are normally targeted together as a complex and may, in fact, form a constitutive complex. A synergistic role of PC1 and tuberin is also suggested by the fact that patients in whom both the *PKD1* and *TSC2* genes are affected have more severe and earlier-onset PKD than patients with *PKD1* mutations alone.

Our results suggest that inappropriate stimulation of mTOR activity may be a common process underlying renal cyst formation. We observed this effect in systems with defects in very diverse proteins: (*i*) ADPKD patients and a mouse model with defective PC1; (*ii*) a mouse model with a defect in polaris, a protein implicated in cilia transport; and (*iii*) a mouse model that overexpresses MAL, a protein implicated in apical membrane targeting (33). Rapamycin was also highly effective in the *bpk* mouse model with a defect in bicaudal C, the homologue of a protein implicated in translational regulation in *Drosophila* (34). Furthermore, defects in the tuberin gene are directly associated with renal cystic disease in humans (7), and increased mTOR activity has been reported in tumor cells derived from a rat model with a defect in tuberin (35). We therefore suggest that mTOR is a downstream effector at a converging point of signaling pathways that involve all of the above gene products. Because rapamycin alone was able to reverse the cystic phenotype in the PKD mouse models, we also conclude that inappropriate activation of the mTOR pathway is likely the sufficient and predominant defect that causes renal cyst formation. It was recently reported that rapamycin improves the cystic phenotype of another model of PKD, the Han:SPRD rat (15, 16). Although the underlying gene defect in this model is still unknown, this finding is consistent with and supports our model that mTOR is a converging point of mechanisms that lead to renal cyst formation.

Even though our retrospective studies on rapamycin-treated ADPKD transplant patients involved only small numbers, the observed significant reduction in renal volumes is highly encouraging and suggestive of a potential for clinical intervention. The impact of ADPKD on patients and the health care system is enormous. Chronic pain, palliative surgery, renal failure, dialysis, and transplantation as well as death are all outcomes of this genetic disease that still has no medical therapy to slow or reverse its progression. The dramatic shortage of donor organs for transplantation makes the search for medical therapy for this disease even more important. This study implicates PC1 as a regulator of mTOR function, shows that mTOR is inappropriately active in ADPKD, and provides evidence that this morbid path may be averted with medical treatment by rapamycin, a drug that is already approved for human use.

Materials and Methods

Reagents. Antibodies were anti-tuberin (C-20) and anti-mTOR (N-19) (Santa Cruz Biotechnology); anti-phospho-mTOR (Ser-2448), anti-phospho-p70 S6 kinase (Thr-389), and anti-phospho-S6 ribosomal protein (Ser-235/236) (Cell Signaling Technology); anti-CD16 (Chemicon); anti-Grp94 (StressGen); anti-GM130 (Transduction Laboratories); anti-acetylated tubulin (Sigma); and anti-Golgin 97 (Molecular Probes). For Western blotting, an ECL kit was used (SuperWest Pico; Pierce).

PC1 Constructs and Generation of Stable MDCK Cell Lines. The cDNAs of membrane-anchored PC1 constructs have been described in ref. 36 and were cloned into pcDNA4/TO (Invitrogen). All fusion proteins contain the extracytoplasmic domain and signal peptide of CD16, the transmembrane domain of CD7 and the full-length cytoplasmic tail of PC1 (FLM-PC1, residues 4077–4302 of human PC1), the N-terminal half of the tail (NTM-PC1, residues 4077–4168), or the C-terminal half of the tail (CTM-PC1, residues 4191–4302). Constructs were transfected into MDCK cells that had been stably transfected for expression of the TET-repressor (37), and stable clones were selected.

Cell-Cycle Analysis. Cells were cultured in the presence or absence of DOX for 24 or 48 h. Cells were harvested, fixed, stained with propidium iodide, and analyzed on a fluorescence-activated cell sorter (Becton Dickinson). The percentages of cells in G_1/G_0, S, and G_2/M were determined by using the program MODFIT (Verity, Sunnyvale, CA).

Cell Proliferation Assay. Cells were cultured in 96-well plates at 10^4 cells per well in the presence or absence of DOX. Cell numbers were evaluated by using the program CYQUANT (Molecular Probes).

Immunohistochemistry and Immunofluorescence Microscopy. Paraffin-embedded tissues were processed and stained as described in ref. 38. Immunofluorescence microscopy on cultured cells was carried out as described in ref. 38. Apoptotic cells in tissue sections were detected by using a TUNEL-based assay (ApopTag; Chemicon).

Coimmunoprecipitation. FLM- and CTM-PC1 MDCK cells were incubated for 16 h in the presence or absence of DOX. Cells were lysed in buffer (50 mM Hepes, 50 mM potassium acetate, 1% 3-[(3-cholamidopropyl)dimethylammonio]-1-propanesulfonate (CHAPS), and protease and phosphatase inhibitors) for 30 min at 4°C. Precleared lysates were incubated with anti-CD16 antibody for

3 h, followed by overnight incubation with protein A-Sepharose at 4°C. Binding proteins were analyzed by Western blot using the indicated antibodies.

Animals. The *orpk*-rescue and the *bpk* mouse models of PKD have been described in refs. 23 and 26. *Bpk* mice were kindly provided by Calvin Cotton (Case Western Reserve University). Tissue sections of MAL-transgenic mice were kindly provided by Ueli Suter (Eidgenössische Technische Hochschule, Zurich) and have been described in ref. 22. The mouse model with a floxed *Pkd1* allele ($Pkd1^{cond/cond}$) has been described (21), and tissue sections from $Pkd1^{cond/cond}$ mice coexpressing the balancer Cre, TgN(balancer1)2Cgn, were used in this study. For rapamycin experiments, mice received no injections or daily i.p. injections of 1.67 or 5 mg/kg rapamycin or vehicle (21.4% DMSO, 21.4% ethanol, and 57.2% saline). For the *orpk*-rescue model, rapamycin was administered starting at postnatal day 150 for a period of 28 days. For the *bpk* model, rapamycin was administered starting at postnatal day 7 for a period of 14 days.

MRI Analysis of Mice. Mice were anesthetized under isoflurane and analyzed in a clinical 1.5T MRI scanner (Sonata; Siemens) using a cylindrical coil (inside diameter, 33 mm) developed in-house. Mice were scanned with a high-resolution 3D True fast-induction steady-state potential (FISP) acquisition [resolution = 260 × 260 × 500 μm, time of repetition (TR)/time of echo (TE) = 10.4/5.2 ms, number of signal averages (NSA) = 4, 24 slices per slab]. Renal volumes were quantified by using the program OSIRIX by measuring slice-by-slice renal areas and summing the individual slice volumes.

Analysis of Mouse Tissues and Blood Samples. After treatment, mice were weighed and anesthetized, and blood was drawn via retroorbital plexus puncture. Blood was separated by centrifugation in a lithium–heparin tube (Becton Dickinson), and plasma blood urea nitrogen levels were determined by using a clinical laboratory service. After cervical dislocation, kidneys were removed, weighed, cut longitudinally, and fixed in 10% neutral-buffered formalin supplemented with 1 mM $MgCl_2$ and 1 mM $CaCl_2$. Kidney samples were embedded in paraffin and sectioned at 5 μm for hematoxylin and eosin (H&E) and immunohistochemical analysis.

Cystic Index Calculations. Representative images of H&E-stained kidneys were acquired. A grid was placed over the images, and the cystic index was calculated as the percentage of grid intersection points that bisected cystic or noncystic areas.

Apoptosis Quantification. To quantify apoptosis in vehicle- and rapamycin-treated *orpk*-rescue ($Tg737^{orpk/orpk}$;*TgRsq*) mutant mice, the total number of identifiable cysts and (*i*) cyst-lining, TUNEL-positive and (*ii*) luminal, TUNEL-positive cells per kidney was counted. An average TUNEL-positive cyst-lining/luminal cell per cyst was generated by dividing the number of cysts by the number of TUNEL-positive cells.

ADPKD Patients. Review of all patients at the Cleveland Clinic who received kidney transplants for ADPKD since January 1996 led us to identify a group of patients with their native polycystic kidneys intact who had received two CT scans, the first within 6 months of the initiation of their immune therapy and the second scan at least 6 months after the first. A single Cleveland Clinic staff radiologist, blinded to our hypothesis and each patient's immunosuppressive group, made all renal dimension measurements by using a standard MagicView 1000 workstation. Noncontrast CT scans were reviewed preferentially by using the multiplanar reformation mode to calculate the maximum distance in each of the three dimensions measured: length, width, and thickness (anteroposterior distance). The maximum length of the kidney was measured at the longest longitudinal segment in the longitudinal plane. The width and thickness were then measured in the transverse plane perpendicular to the longitudinal plane and orthogonal to one another. Renal volumes were calculated by using an ellipsoid formula as described in ref. 27. Patients were divided into two groups: The rapamycin group received rapamycin as their main immunosuppressive agent in possible combination with mycophenylate and prednisone. The nonrapamycin control group received cyclosporine as their main immunosuppressive agent in possible combination with azothioprine, mycophenylate, and prednisone. Native polycystic kidney volume changes over time were calculated, and the two groups were compared.

Statistical Analysis. Statistical analyses were performed by using unpaired Student's t test. $P < 0.05$ was considered statistically significant.

We thank Brian Herts for radiological analyses, Paul Elson for statistical analyses, Xin Li for initial experiments, and Calvin Cotton and Ueli Suter for reagents and animals. This work was supported by National Institutes of Health Grants R01-DK62338 (to T.W.) and P50-DK57306 (to N.S.M.), an American Heart Association Scientist Development grant (to S.H.L.), and the generous support of Martha and Jerry Jarrett (to T.W.).

1. Torres, V. E. & Harris, P. C. (2003) *Nefrologia* **23,** 14–22.
2. Igarashi, P. & Somlo, S. (2002) *J. Am. Soc. Nephrol.* **13,** 2384–2398.
3. Wilson, P. D. (2004) *N. Engl. J. Med.* **350,** 151–164.
4. Sutters, M. & Germino, G. G. (2003) *J. Lab. Clin. Med.* **141,** 91–101.
5. Ong, A. C. & Harris, P. C. (2005) *Kidney Int.* **67,** 1234–1247.
6. Nauli, S. M., Alenghat, F. J., Luo, Y., Williams, E., Vassilev, P., Li, X., Elia, A. E., Lu, W., Brown, E. M., Quinn, S. J., *et al.* (2003) *Nat. Genet.* **33,** 129–137.
7. Sampson, J. R., Maheshwar, M. M., Aspinwall, R., Thompson, P., Cheadle, J. P., Ravine, D., Roy, S., Haan, E., Bernstein, J. & Harris, P. C. (1997) *Am. J. Hum. Genet.* **61,** 843–851.
8. Narayanan, V. (2003) *Pediatr. Neurol.* **29,** 404–409.
9. Zhang, Y., Gao, X., Saucedo, L. J., Ru, B., Edgar, B. A. & Pan, D. (2003) *Nat. Cell Biol.* **5,** 578–581.
10. Pan, D., Dong, J., Zhang, Y. & Gao, X. (2004) *Trends Cell Biol.* **14,** 78–85.
11. Li, Y., Corradetti, M. N., Inoki, K. & Guan, K. L. (2004) *Trends Biochem. Sci.* **29,** 32–38.
12. Fingar, D. C., Salama, S., Tsou, C., Harlow, E. & Blenis, J. (2002) *Genes Dev.* **16,** 1472–1487.
13. Burnett, P. E., Barrow, R. K., Cohen, N. A., Snyder, S. H. & Sabatini, D. M. (1998) *Proc. Natl. Acad. Sci. USA* **95,** 1432–1437.
14. Inoki, K., Corradetti, M. N. & Guan, K. L. (2005) *Nat. Genet.* **37,** 19–24.
15. Tao, Y., Kim, J., Schrier, R. W. & Edelstein, C. L. (2005) *J. Am. Soc. Nephrol.* **16,** 46–51.
16. Wahl, P. R., Serra, A. L., Hir, M. L., Molle, K. D., Hall, M. N. & Wüthrich, R. P. (2005) *Nephrol. Dial. Transplant.*
17. Scheffers, M. S., van Der Bent, P., Prins, F., Spruit, L., Breuning, M. H., Litvinov, S. V., de Heer, E. & Peters, D. J. (2000) *Hum. Mol. Genet.* **9,** 2743–2750.
18. Peters, D. J., van de Wal, A., Spruit, L., Saris, J. J., Breuning, M. H., Bruijn, J. A. & de Heer, E. (1999) *J. Pathol.* **188,** 439–446.
19. Xu, L., Sterner, C., Maheshwar, M. M., Wilson, P. J., Nellist, M., Short, P. M., Haines, J. L., Sampson, J. R. & Ramesh, V. (1995) *Genomics* **27,** 475–480.
20. Long, X., Lin, Y., Ortiz-Vega, S., Yonezawa, K. & Avruch, J. (2005) *Curr. Biol.* **15,** 702–713.
21. Piontek, K. B., Huso, D. L., Grinberg, A., Liu, L., Bedja, D., Zhao, H., Gabrielson, K., Qian, F., Mei, C., Westphal, H. & Germino, G. G. (2004) *J. Am. Soc. Nephrol.* **15,** 3035–3043.
22. Frank, M., Atanasoski, S., Sancho, S., Magyar, J. P., Rulicke, T., Schwab, M. E. & Suter, U. (2000) *J. Neurochem.* **75,** 1927–1939.
23. Brown, N. E. & Murcia, N. S. (2003) *Kidney Int.* **63,** 1220–1229.
24. Sabers, C. J., Martin, M. M., Brunn, G. J., Williams, J. M., Dumont, F. J., Wiederrecht, G. & Abraham, R. T. (1995) *J. Biol. Chem.* **270,** 815–822.
25. Lorenz, M. C. & Heitman, J. (1995) *J. Biol. Chem.* **270,** 27531–27537.
26. Nauta, J., Ozawa, Y., Sweeney, W. E., Jr., Rutledge, J. C. & Avner, E. D. (1993) *Pediatr. Nephrol.* **7,** 163–172.
27. Fick-Brosnahan, G. M., Belz, M. M., McFann, K. K., Johnson, A. M. & Schrier, R. W. (2002) *Am. J. Kidney Dis.* **39,** 1127–1134.
28. Flechner, S. M., Goldfarb, D., Modlin, C., Feng, J., Krishnamurthi, V., Mastroianni, B., Savas, K., Cook, D. J. & Novick, A. C. (2002) *Transplantation* **74,** 1070–1076.
29. Gingras, A. C., Raught, B. & Sonenberg, N. (2001) *Genes Dev.* **15,** 807–826.
30. Luan, F. L., Ding, R., Sharma, V. K., Chon, W. J., Lagman, M. & Suthanthiran, M. (2003) *Kidney Int.* **63,** 917–926.
31. Harada, H., Andersen, J. S., Mann, M., Terada, N. & Korsmeyer, S. J. (2001) *Proc. Natl. Acad. Sci. USA* **98,** 9666–9670.
32. Kleymenova, E., Ibraghimov-Beskrovnaya, O., Kugoh, H., Everitt, J., Xu, H., Kiguchi, K., Landes, G., Harris, P. & Walker, C. (2001) *Mol. Cell* **7,** 823–832.
33. Cheong, K. H., Zacchetti, D., Schneeberger, E. E. & Simons, K. (1999) *Proc. Natl. Acad. Sci. USA* **96,** 6241–6248.
34. Cogswell, C., Price, S. J., Hou, X., Guay-Woodford, L. M., Flaherty, L. & Bryda, E. C. (2003) *Mamm. Genome* **14,** 242–249.
35. Kenerson, H. L., Aicher, L. D., True, L. D. & Yeung, R. S. (2002) *Cancer Res.* **62,** 5645–5650.
36. Arnould, T., Sellin, L., Benzing, T., Tsiokas, L., Cohen, H. T., Kim, E. & Walz, G. (1999) *Mol. Cell. Biol.* **19,** 3423–3434.
37. Low, S. H., Li, X., Miura, M., Kudo, N., Quinones, B. & Weimbs, T. (2003) *Dev. Cell* **4,** 753–759.
38. Weimbs, T., Low, S. H., Li, X. & Kreitzer, G. (2003) *Methods* **30,** 191–197.

Shillingford *et al.* 10.1073/pnas.0509694103.

Supporting Information

Files in this Data Supplement:

Supporting Figure 6
Supporting Figure 7
Supporting Table 1

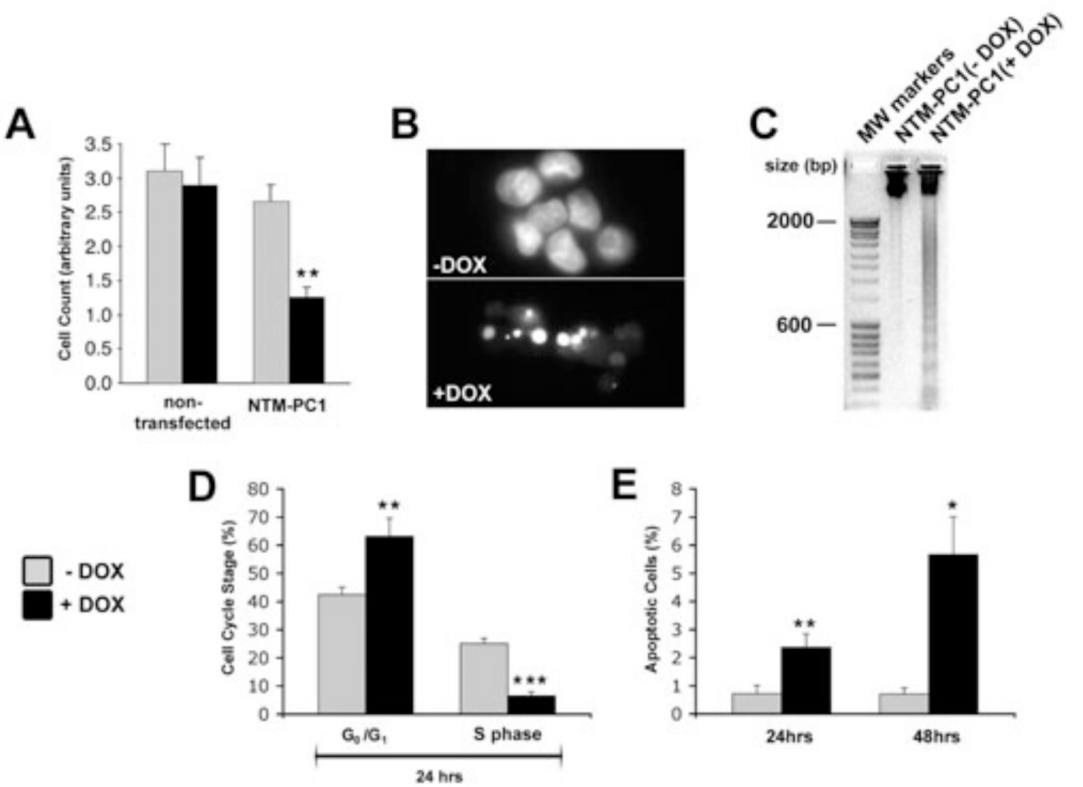

Fig. 6. The N-terminal cytoplasmic domain of PC1 induces cell cycle arrest and apoptosis. (*A* and *B*) Identical numbers of MDCK cells stably transfected for the membrane-anchored N-terminal cytoplasmic domain of PC1 (NTM-PC1) were cultured in the presence or absence of DOX for 48 h. (*A*) Numbers of cells attached after this time were quantified and are expressed in arbitrary units. Note that induction of expression of NTM-PC1 resulted in a significant decrease of cell numbers. (*B*) DNA of detached cells was stained with DAPI to reveal typical condensed and fragmented apoptotic nuclei in NTM-PC1-expressing cells (+DOX). (*C*) The DNA of attached cells was isolated and analyzed by agarose-gel electrophoresis. Note that induction of NTM-PC1 expression results in DNA-laddering, indicative of apoptosis. (*D* and *E*) Cell cycle analysis of attached cells was carried out by FACS in induced and noninduced NTM-PC1 cells. (*D*) Note that at 24 h, cells exhibited a significant increase in G_1/G_0 cell cycle and a significant reduction of cells in S-phase. (*E*) The fraction of apoptotic cells is significantly increased after induction of expression of NTM-PC1 for 24 and 48 h. *, $P < 0.05$; **, $P < 0.01$; ***, $P < 0.001$.

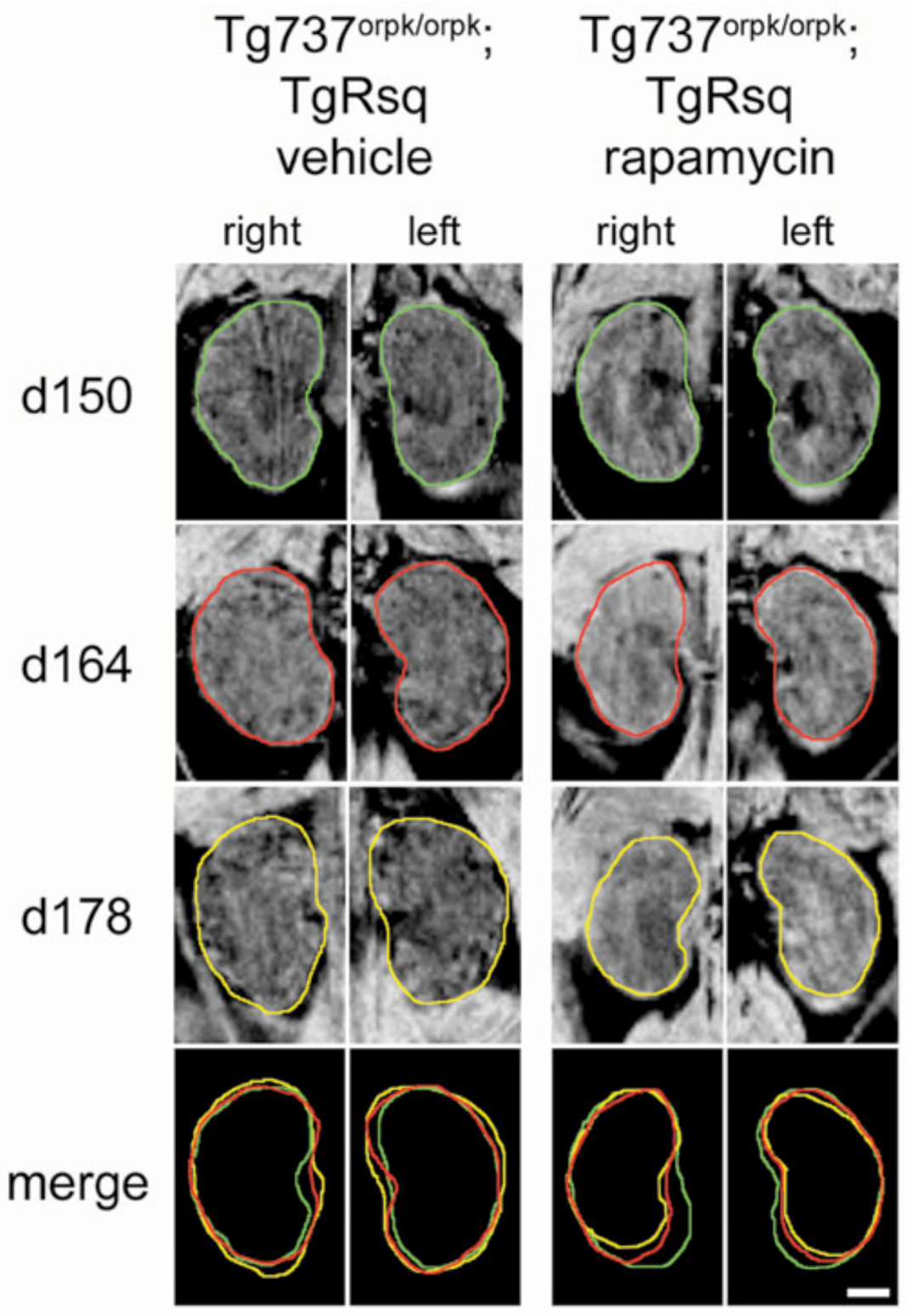

Fig. 7. Analysis of renal volume changes by MRI scanning. Vehicle- and rapamycin-treated *orpk*-rescue (*Tg737*^{orpk}/*orpk*;*TgRsq*) mutant mice were subjected to MRI scanning at day 150, day 164, and day 178. The maximum slice volume for each kidney was determined by using the analysis program OSIRIX. The outline of each kidney at each time point was traced as shown and is represented as a merged image. Note the visual increase in maximal slice volume in vehicle-treated *orpk*-rescue mutant mice vs. the decrease in maximal slice volume in rapamycin-treated *orpk*-rescue mutant mice over the time course of the study. Cystic structures, evident as black areas within the kidney parenchyma, are significantly fewer in rapamycin-treated *orpk*-rescue mutant mice vs. vehicle-treated *orpk*-rescue mutant mice. (Scale bar, 3 mm.)

Table 1. Calculated CT renal volume of native polycystic kidneys in kidney transplant patients receiving rapamycin vs. nonrapamycin immunosuppression

Rapamycin Treatment						
Patient	Kidney	Initial renal volume, ml	Final renal volume, ml	Volume change, ml	Volume % change	Follow-up, months
1	A	1,081	639	–442	–40.9%	23
	B	1,069	736	–333	–31.2%	23
2	C	623	535	–88	–14.1%	44
	D	974	757	–217	–22.3%	44
3	E	1,288	937	–351	–27.3%	11
	F	1,788	1,344	–444	–24.8%	11
4	G	1,802	1,572	–230	–12.8%	14
Averages		1,232	931	–301	–24.8%	24
Analysis		Total % Volume Change:			–24.8% ± 9.7% (P =.001)	
		% Volume Change per Month:			–1.4% ± 0.8% (P =.005)	
Nonrapamycin treatment						
Patient	Kidney	Initial renal volume, ml	Final renal volume, ml	Volume change, ml	Volume % change	Follow-up, months
5	M	1,621	1,406	–215	–13.3%	22
	N	1,174	1,251	77	6.6%	22
6	O	464	459	–5	–1.1%	69
	P	735	575	–160	–21.8%	69
7	Q	1,949	1,689	–260	–13.3%	20
Averages		1,189	1,076	–113	–8.6%	40
Analysis		Total % volume change			–8.6% ± 11.2% (P = 0.16)	
		% Volume change per month:			–0.3% ± 0.4% (P = 0.22)	

Volumes of native polycystic kidneys in human transplant patients were calculated by using an accepted ellipsoid volume formula from dimensions measured retrospectively on patient CT scans. Initial volumes were calculated from CT scans performed no more than 12 months prior to 5 months after receiving a kidney transplant and initiating immune-suppression therapy. Final volumes of these same native kidneys were also measured retrospectively from a CT scan performed at least 11 months after transplantation. The follow-up period between the two scans was measured and is shown as follow-up in months. Patients who received rapamycin as part of their immune suppression were placed in the rapamycin treatment group and those that did not were placed in the nonrapamycin treatment group. Volume changes for the kidneys were then analyzed statistically within groups by using a paired t-test and between the two groups by using an unpaired t-test.